HCCI engine CFD simulations: Influence of intake temperature, cylinder wall temperature and the equivalence ratio on ignition timing

Kezhuo Wang

Advisor: Dr. Seung Hyun Kim

An Undergraduate Honors Thesis

Submitted to the Department of Mechanical Engineering at

The Ohio State University

Spring, 2018

Abstract

To meet the increasingly stringent emission standards, the automotive industry is actively searching for means to improve the efficiency of an internal combustion engine. One promising solution is a homogeneous charge compression ignition (HCCI) engine which has shown potential in achieving high fuel efficiency while maintaining low emission. However, there remain several challenges to commercialize the HCCI engine due to the nature of its working principle. Since the HCCI engine relies purely on compression to achieve ignition, controlling the ignition timing is much harder than in spark-ignition (SI) engines and diesel engines. This study focuses on simulating the ignition and combustion processes inside the HCCI engines and investigating the impacts of different operating conditions, such as intake temperature, the equivalence ratio, and cylinder wall temperature. The study is conducted by using the CONVERGE Computational Fluid Dynamics (CFD) software which allows robust and accurate engine simulation. Current progress shows that lower intake temperature retards the combustion timing and decreases combustion efficiency. Results from CFD simulations are compared to experimental data for a research HCCI engine. Trends observed in the simulations show good agreement with those in the experiments in terms of the impact of different intake temperatures. Further investigation shows that lower cylinder wall temperature retards ignition timing and extends ignition duration. The mixture temperature is found to be more sensitive to the cylinder wall temperature than the intake temperature. When lean mixtures with the equivalence ratio smaller than 1 are considered, the ignition of iso-octane is advanced as it's equivalence ratio increases.

Acknowledgements

Foremost, I would like to thank my thesis advisor, Dr. Seung Hyun Kim for the continuous support. I am grateful to Dr. Kim for enlightening me the first glance of research. He was always willing to listen to my questions and clear my doubts. This study would not have existed without his guidance and support. I could not have imagined a better advisor and mentor for my study.

My sincere thanks to the PhD students in Computational Combustion and Energy research group: Yunde Su, Weibo Zheng, and Wei Wang for giving me advices on conducting simulations and pursue in independent research.

Last but not least, I would like to thank my parents for nourishing and supporting me throughout my life. None of my accomplishments would have been possible without them. Thank you.

Table of Contents

List of figures

List of tables

1. Introduction

Automotive is one of the fastest growing industry in the world. It is estimated that the number of vehicles owned throughout the world will increase from 700 million to approximately 2 billion by 2050. Although the electrification of vehicles is on the horizon, cars with internal combustion engines are expected to maintain its significant portion of the market share [1,2]. There are mainly two types of internal combustion engines that are commercially available today: SI engines and diesel engines. SI engines are effective at minimizing urban pollutants, while diesel engines are effective at minimizing CO_2 emission. Furthermore, diesel engines combined with modern aftertreatment technologies are more effective at minimizing urban pollutants than SI engines do. However, the aftertreatment technologies are expensive [3]. With the expectations of increasing vehicle ownerships and stringent emission standards [4], improvements and alternatives to the aforementioned engines are being actively researched by automakers.

Homogenous charged combustion ignition (HCCI) engines offer an alternative to SI and diesel engines. In theory, an HCCI engine has superior potential for achieving high part load fuel conversion efficiency. Similar to diesel engines, HCCI engines utilize the heat converted from the mechanical work during the compression stroke to achieve high efficiency operation. Furthermore, HCCI engines use a lean well-mixed air-fuel mixture to enable low emissions of soot, NO_x and particulate matters [3, 5].

HCCI engines have two defining characteristics. The first is how the air-fuel mixture is prepared. As the name suggests, in HCCI engines, the homogeneous mixture of fuel and air is charged before combustion. The most common methods to achieve it are port fuel injection

(PFI) and direction injection (DI). The difference between these two methods is that PFI sprays the fuel into the intake manifold to mix it with intake air while DI sprays the fuel directly into the engine cylinders. Both methods are effective in producing relatively homogenous air-fuel mixtures. This is in contrast to diesel engines, where the fuel is directly injected into the cylinder at the end of the compression stroke. The second is how the mixture is ignited. Different from SI engines, the ignition of the air-fuel mixture in the engine cylinder relies on chemistry. During each cycle, the temperature of the air-fuel mixture inside the cylinder rises due to the mechanical work done during the compression stroke, and the combustion timing and heat release rates are solely controlled by chemical kinetics under given in-cylinder conditions.

Nevertheless, HCCI engines must overcome two challenges before commercialization: 1) accurate control of combustion timing, and 2) achieve high load capability. Since HCCI engines use compression to achieve ignition, the mixture can auto-ignite and combust simultaneously at multiple locations inside the combustion chamber. As a result, combustion in HCCI engines is typically significantly faster than in SI and diesel engines, where flame propagation speeds or mixing and vaporization rates control the heat release rates [3]. During high load operations, the overly high heat release rate and pressure rise rate caused by excessively rapid combustion in the engine cylinder has been found to be the cause of the knocking or ringing behavior which inhibits HCCI engine's high load capability [6].

Since the combustion timing of an HCCI engine is governed by chemical kinetics, the temperature of the charged mixture plays a critical role in controlling the combustion processes in an HCCI engine. Furthermore, since the air-fuel mixture enters the engine cylinder during

the intake stroke, the temperature of the mixture is also affected by the temperature of cylinder walls through heat transfer. Hence, this study focuses on investigating the impact of intake temperature, cylinder wall temperature and the equivalence ratio on the combustion timing and heat release in an HCCI engine. Computational simulations using a commercial software, Converge CFD, are performed for a single-cylinder research HCCI engine.

2. Computational method

CFD simulation was first carried out to emulate part of the experiments previously described by Lawler et al. [7]. Then, multiple simulations with different operating parameters such as intake temperature, cylinder wall temperature and the equivalence ratio were conducted to investigate the parameters' impacts on combustion processes.

The aforementioned study used a single cylinder Ricardo Hydra engine as the experimental setup. The engine head was a four-valve, pent-roof design with a centrally located spark plug and a side mounted direct injector. The study used a method known as Thermal Stratification Analysis (TSA) to calculate and analysis the unburned temperature distribution based on temperature measurements. Hence the study was able to conduct without the aid of optically-accessible engines. To measure instantaneous surface temperature and pressure during the experiment, the engine head was machined to install transducers and probes.

The part of study this project tried to emulate was the premixed positive valve overlap combustion phasing study. In this part of the experiment, the selected fuel in the experiment was 87 AKI research grade unoxygenated gasoline whose lower heating value was reported to

be 44.3 MJ/kg. The air-fuel mixture was prepared by mixing upstream in a fuel vaporizer before entering the intake plenum [7]. To adapt the experiment into CFD simulations, two simulation decisions were made. First, since the specification of the fuel vaporizer was not specified by the authors, the premixed method used in the CFD simulation was PFI. To simulate the mixing process, the same amount of fuel was injected in the intake manifold -400 crank angles degrees before intake valve open. The injection duration was 10 crank angles degrees. Second, instead of using 87 AKI gasoline as the fuel for simulation, pure iso-octane was selected as the fuel in simulation. First, iso-octane's lower heating value is 44.3 MJ/kg [8] which is close to 87 AKI gasoline's lower heating value (43.13 MJ/kg) [7]. Second, both iso-octane and 87 AKI gasoline are single stage ignition fuel. Therefore, combustion of iso-octane has similar combustion characteristics when compared with the fuel used by the study conducted by Lawler et al., while there is a difference in the ignition delay.

The CFD simulation cases were setup in CONVERGE CFD. CFD calculations for the simulation case were conducted using a finite volume numerical method within CONVERGE CFD [9-11]. Based on the key dimensions provided in the paper done by Lawler et al [7], engine surface was first created in computer-aided design software and imported in CONVERGE. It's worth mentioning that since the study focused on investigating the impacts of parameters such as intake temperature and cylinder wall temperature, only a part of the engine's intake manifold, exhaust manifold and cylinder block was created. The created geometry was subsequently mapped onto an orthogonal grid whose base grid size was determined by a convergence study to be 4mm. A converge study was conducted to determine the optimal grid size. Then, CONVERGE used the created engine geometry to cut the cells that

were intersected by the engine surface. Further mesh refinement was done in CONVERE with two methods: cell scaling (fixed embedding) and adaptive mesh refinement (AMR). Fixed embedding enables the user to refine the mesh at specified locations and times. In the simulation, fixed embedding was enabled near a fuel injector, an intake valve and an exhaust valve. AMR automatically adapted the mesh based on fluctuating and moving conditions [9]. AMR was enabled for the spatial gradients in temperature and velocity. Mesh refinements enabled higher local resolution and accurate simulation results when more cells were needed. For example, when the velocity of flow was changing rapidly due to moving surfaces or narrowing channels, finer mesh was required to accurately simulate the complex phenomena. Furthermore, enabling local mesh refinement in CONVERGE improved computational efficiency while maintaining the accuracy of simulation. Fixed embedding was enabled near fuel injector, The essential simulation parameters are listed in Table 1.

Table 1. Essential simulation parameters

Engine type	4 valve, 4 stroke, single cylinder
Initial conditions	-400 CAD at 1000 K and 180000 Pa
Bore/stroke	86/94.6 mm
Displacement	0.550 L
Connecting rod length	152.2 mm
Compression ratio	12.8:1
Intake valve open/intake valve close	329.5 degree/-141.5 degree
Exhaust valve open/exhaust valve close	133.5 degree/-351.5 degree
Piston	Flat-topped
Fuel preparation	One injector with four nozzles (orifice diameters: 2×0.25 mm diameter, 2×0.2 mm), start of injection: -400 CAD before top dead center (TDC), injection duration: 10 CAD
Fuel type	iso-octane

CONVERGE offers a wide array of numerical techniques and models for physical and chemical processes. The first aspect considered when setting up simulation cases was turbulence modelling. Turbulence in combustion chamber significantly increases the rate of mixing of air-fuel mixture, energy and momentum. Three types of turbulence model are available in CONVERGE: Reynolds-Averaged Navier-Stokes (RANS) turbulence model, Large Eddy Simulation (LES) and Detached Eddy Simulation (DES). The RANS model is widely used in CFD simulation for computational efficiency. Data collected from turbulent reacting flow experiments had been compared with simulation with the RANS model by a study conducted by Anthony and Moder [12]. The simulation results were reported to be

showing good agreements with experiments. Furthermore, studies conducted by A. d'Adamo et al. [13] had shown that the combustion simulation results obtained using the RANS model was accurate enough to be used to predict the knocking behavior in internal combustion engine. However, the RANS model is limited to only be able to give insights into the average behavior of the in-cylinder flow. In contrast, the LES model and DES model are useful to give insights into the cycle-to-cycle variations inside the engine cylinder at the cost of computational efficiency. However, this is only meaningful when multiple engine cycles are simulated. Additionally, it has been reported [14] that at least 25 cycles are required for mean value predictions. Therefore, to improve the computational efficiency, the Reynolds-Averaged Navier-Stokes (RANS) turbulence model was used to model the turbulent flow and account for the mixing effects of turbulent flow.

To accurately model the fuel spray, the drop drag was first considered. CONVERGE CFD offers three ways to calculate the drag experienced by fuel droplets: dynamic drag model, no drag model and perfect sphere model. The first option, dynamic drag model, determines the drag coefficient dynamically by accounting for the effects of droplet distortion [15]. The second option, no drag model, assumes the fuel droplets experience no drag force. The third option, perfect sphere model, determines the drag coefficient by assuming the shape of fuel droplets is perfect spheres. It's important to point out that as the initially spherical droplets moves through gases, the shape of droplets will distort and result in change in different drop drag coefficient. Therefore, the dynamic drag model, which accounts for the effect of droplet distortion, is used to determine the drop drag coefficient [9].

Second, to simulate the spray breakup, Kevin-Helmholtz and Rayleigh-Taylor breakup

length models (KH-RT) are used to simulate the breakup of the fuel droplet. Study conducted by Som et al. [16] had shown that these two models predicted fuel spray accurately. CONVERGE used both breakup models concurrently to check if the droplet breaks up.

Third, the collision and coalescence of droplets were considered. CONVERGE CFD offers three ways to process the interaction between fuel droplets: no collision model, O'Rourke collision model and no time counter (NTC) model developed by Schmidt and Rutland [17]. The no collision model was excluded from consideration since the outcomes of droplets collision are crucial for accurate simulation [9]. The O'Rourke collision model has long been the standard of droplet collision and coalescence simulation [18]. However, when comparing the model with the NTC model, it's reported that the computational cost of the NTC model is significantly smaller than the O'Rourke model while maintaining accurate results. The report further demonstrates that the computational cost of the NTC model increases linearly with the number of parcels while the costg of O'Rourke model increases quadratically. Since the NTC model enables low computational costs at larger numbers of parcels, the NTC model is used to model the collision and coalescence of droplets.

Fourth, among the three options (wall film model, rebound/slide model, drop vanish model) offered in CONVERGE, the droplet-wall interaction was modeled using the wall film model. In the simulation, the fuel was injected in the intake manifold to mix with intake air. Therefore, it was necessary to include the film modeling and interactions between droplets and film. Since both the rebound/slide model and the drop vanish model didn't include the modeling of film and droplet-film interaction. The wall film model was selected.

The chemistry model reported by Liu et al. [19] was used to describe the combustion

chemistry. A total of 44 species and 139 reaction equations were included in the reaction model. The model was validated against various experimental data and showed good agreement with the data. The model was defined in the CHEMKIN format and solved using CONVERGE's SAGE solver. The species' physical properties such as specific heat, density and viscosity were also defined in the simulation model. Mesh convergence studies were conducted for four different mesh sizes. The mesh convergence studies showed that a base mesh size of 4mm was best suited for the simulation. Referring to Figure 1, the results converged at a base mesh size of 4mm. An example of adaptive mesh refinement during an intake stroke is shown in Figure 2. Figure 2 illustrates the mesh refinement done by fixed embedding near the injector and AMR. The maximum number of cells was near 157000 around the end of a compression stroke. Computations were conducted in parallel on 48 cores. On average, each case took 85 hours to be solved.

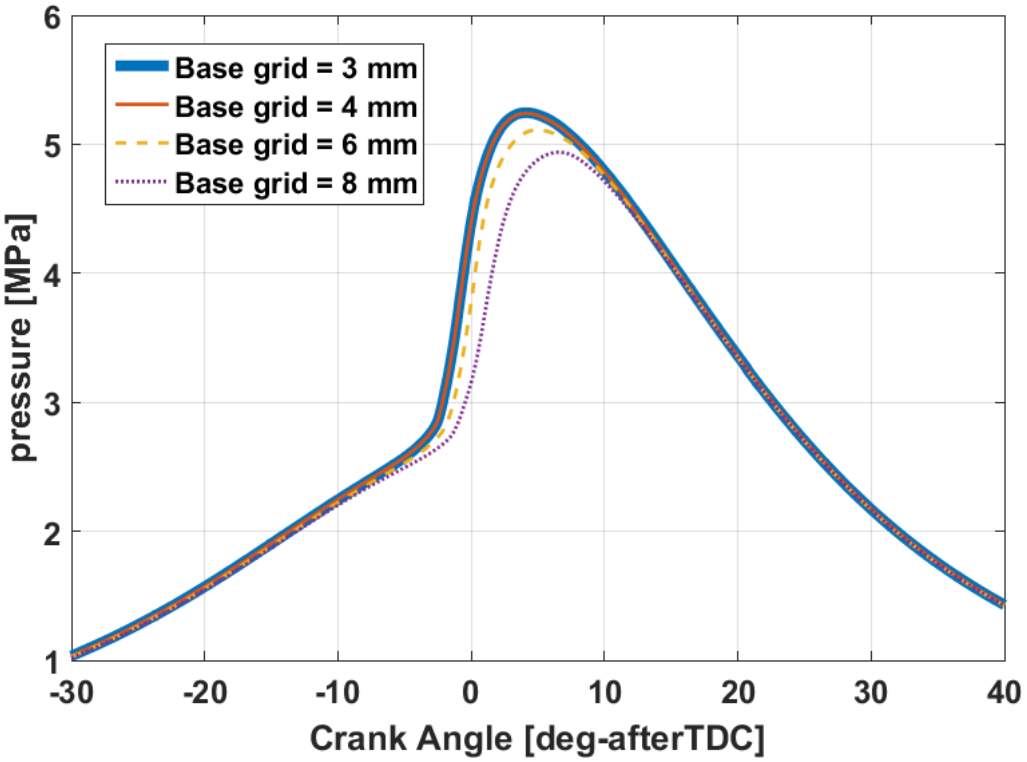

Figure 1. Mesh convergence tests demonstrating the mesh converges at the base grid size of 4mm

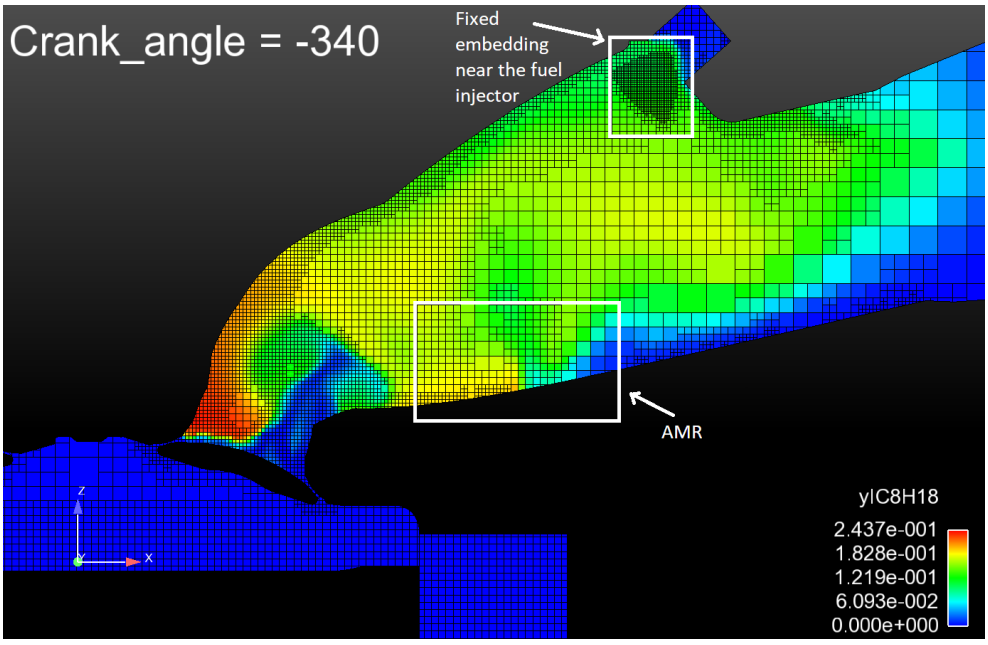

Figure 2. Adaptive mesh refinement during an intake stroke

3. Results and discussion

3.1. Experimental case

The experiments carried out by Lawler et al. in the premixed positive valve overlap combustion phasing study showed that: 1) Lower intake temperature and lower equivalence ratio led to lower burn rate and later combustion phasing. 2) Maximum temperature and temperature distribution in combustion chamber at TDC increased with higher intake temperature [7].

CFD simulation was carried out to emulate the experiment. However, due to the uncertainty in the experimental conditions, it was difficult to make a quantitative comparison. The effects of intake temperature and equivalence ratio were investigated and discussed in section 3.2 and 3.4. The trends obtained from the simulations agreed with the trends reported in the study.

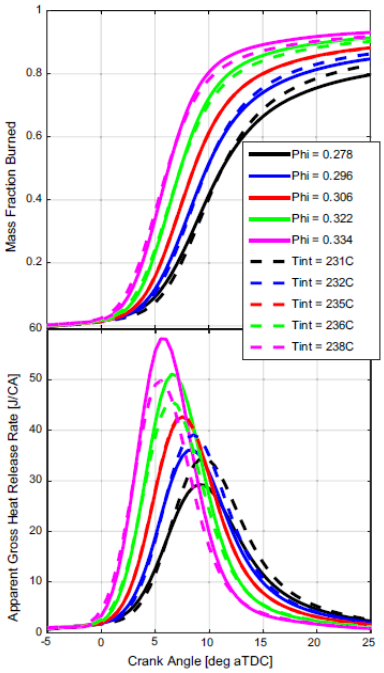

Figure 3. Mass fraction burned curves and heat release rates from the experiment done by Lawler et al. [7]

3.2 Effects of intake temperature

Figure 4 shows simulated average temperature inside the combustion chamber at five different intake temperatures. It clearly illustrates that the combustion phasing is delayed as intake temperature decreases. To better illustrates this, the crank angles before TDC of different combustion phasing are recorded in Table 2. Table 2 shows that as intake temperature decreased from 528 K to 488 K, ignition timing was delayed. The crank angles at 10% heat release (CA10) was delayed from -3.87 crank angles degrees (CAD) after TDC to 0.20 CAD after TDC. Furthermore, the crank angles at 90% heat release (CA90) was delayed from 2.05 CAD to 8.16 CAD. The combustion duration, defined as the crank angles difference between CA10 to CA90, extended from 5.92 CAD to 8.36 CAD.

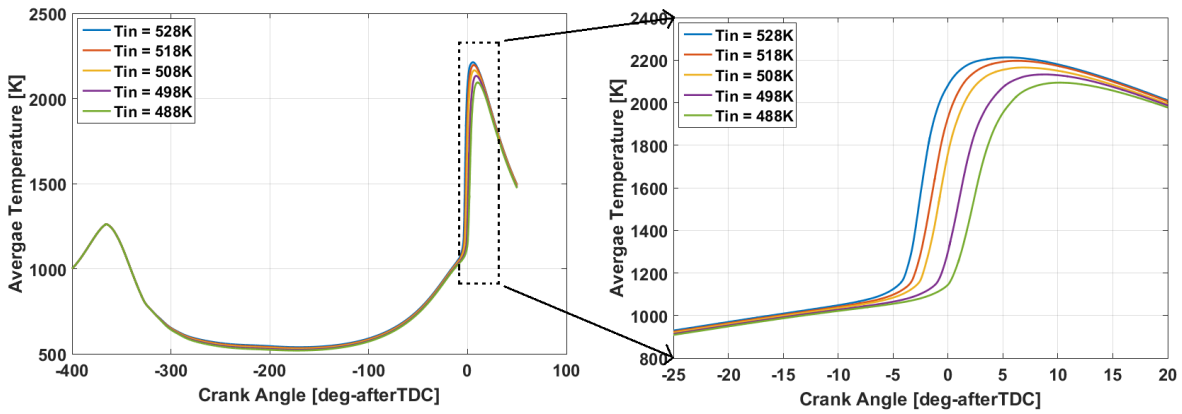

Figure 4. Effects of intake temperature on the evolution of the mixture temperature inside a cylinder

Table 2. Crank angles at different combustion phasing at five different intake temperatures

Intake temperature (K)	CA10 (crank angles)	CA50 (crank angles)	CA90 (crank angles)	Combustion duration (crank angles)	Total Heat release (J)
528	-3.87	-2.08	2.05	5.92	596.3
518	-3.09	-0.95	3.09	6.18	595.6
508	-2.46	-0.28	4.39	6.85	594.7
498	-0.88	1.56	6.29	7.17	594.7
488	0.20	2.90	8.16	8.36	591.1

Furthermore, lower burning rates were observed in the simulation. Figure 5 shows the simulated mass fraction of fuel burned vs. time and fuel burning rates vs. time. The figure shows a strong correlation between intake temperature and fuel burning rates. As the intake temperature decreases, the maximum fuel burning rate decreases while the combustion duration extends as it was noted in Table 2. The trends observed in simulation matched well with those in the experiment conducted by Lawler et al [7].

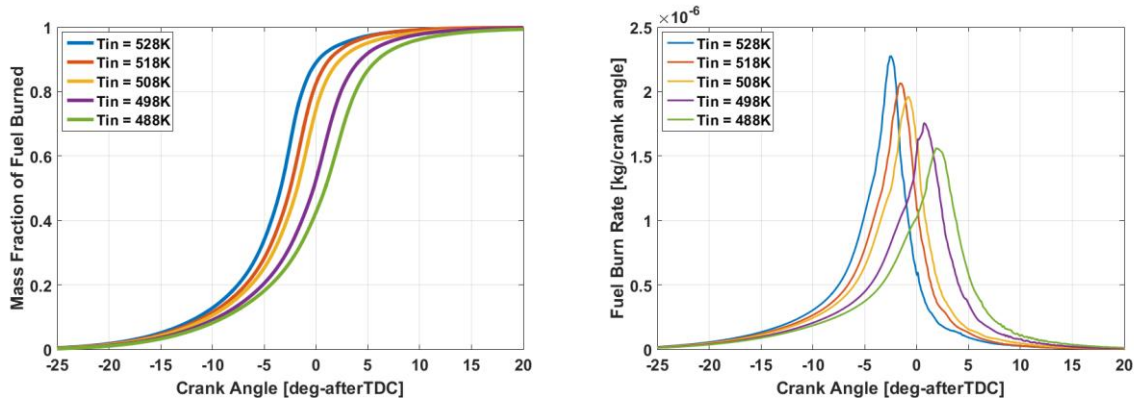

Figure 5. Effects of intake temperature on the evolution of mass fraction of fuel burned and fuel burning rate

3.3 Effects of cylinder wall temperature

To investigate the impact of different temperature of the cylinder wall, the temperature of the wall was adjusted in the CONVERGE CFD's simulation setup. Five different cylinder wall temperature: 453 K, 423 K, 393 K, 363 K and 303 K were tested. The intake temperature for these cases were 508K.

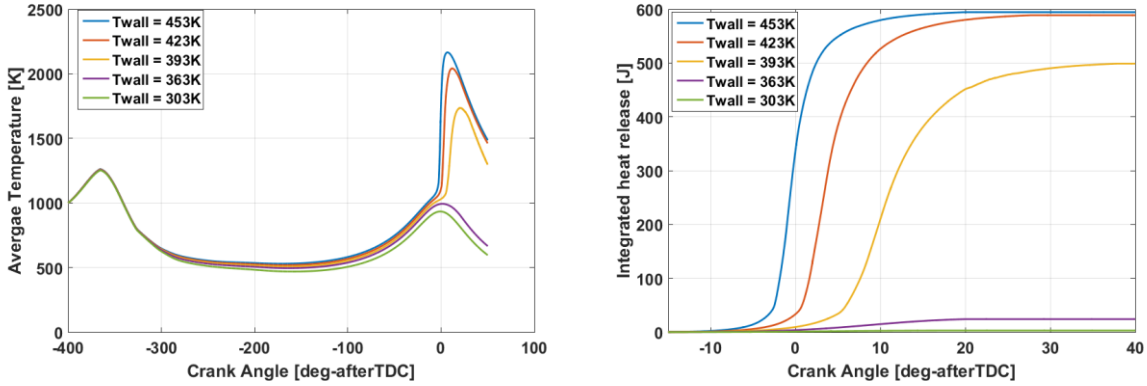

Figure 6. Effect of cylinder wall temperature on the evolution of the mixture temperature and heat release

Table 3. Crank angles at different combustion phasing at five different cylinder wall temperatures

Cylinder wall temperature (K)	CA10 (crank angles)	CA50 (crank angles)	CA90 (crank angles)	Combustion duration (crank angles)	Total Heat release (J)
453	-2.46	-0.28	4.39	6.85	594.7
423	0.96	3.74	10.29	9.33	588.7
393	5.92	10.83	19.83	13.91	498.8
363	-2.17	7.93	16.13	18.30	24.04
303	N/A	N/A	N/A	N/A	N/A

Figure 6 illustrates that the maximum temperature in the engine cylinder decreases as the cylinder wall temperature decreases. Likewise, other trends observed in section 3.1's simulation results are also observed. As it is shown in Table 3, combustion duration extended and ignition timing retarded at lower cylinder wall temperature. Additionally, low heat release rates were observed at an initial cylinder wall temperature of 363 K and 303 K. Hence, engine misfire was observed when the temperature of the cylinder wall was at these two temperatures. Since the auto-ignition process of HCCI engine is governed by chemical kinetics, the heat transfer between cylinder wall and air-fuel mixture plays a critical role on controlling combustion processes. Figure 7 shows the temperature at the beginning (CA10) and the end

(CA90) of combustion at different intake temperatures and cylinder wall temperatures. In Figure 7, the two lines on the left illustrate the impacts of changes in the cylinder wall temperature. The blue line in the figure has a higher slope than the red line's which indicates that the temperature of the charged mixture's temperature at the beginning of combustion is more sensitive to the changes in cylinder wall temperature than changes in intake temperature. Consequently, with lower mixture temperature, the combustion phasing is retarded and the total heat release is reduced.

Since the air-fuel mixture enters the engine cylinder at 329.5 CAD before TDC, the heat transfer between the engine cylinder wall and the charged mixture is significant enough to alter the mixture temperature at the beginning of combustion and influence the combustion. Moreover, as the cylinder wall temperature decreases, the temperature difference between the cylinder wall and the air-fuel mixture increases, which accelerates the heat transfer and results in higher temperature sensitivity.

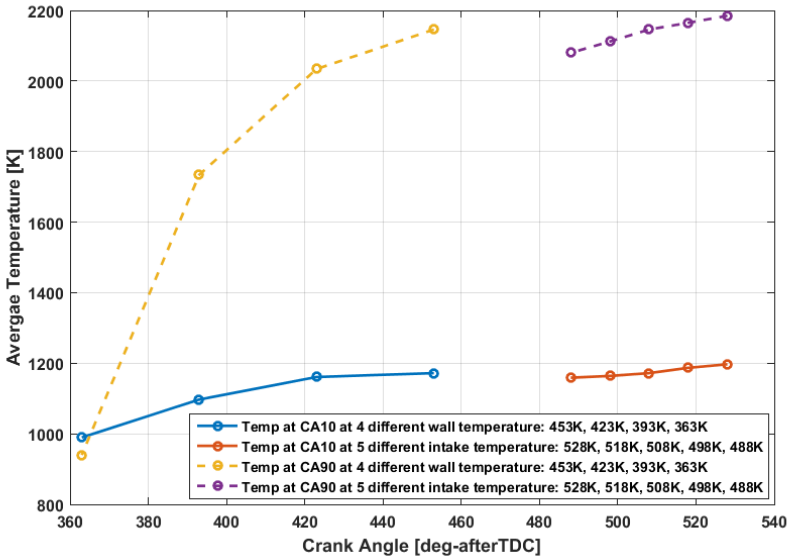

Figure 7. Effects of intake temperature and cylinder wall temperature on the fuel burning rates at the start of ignition (CA10) and near the end of ignition (CA90).

3.4 Effects of the equivalence ratio

To investigate the impact of different equivalence ratios, the amount of fuel injected was adjusted in the CONVERGE CFD's simulation setup. Three different equivalence ratios are tested: 0.586, 0.446, 0.303. The equivalence ratio is calculated using the equation below.

$$Equivalence\ ratio = \frac{\frac{mole\ of\ fuel\ in\ cylinder}{mole\ of\ oxygen\ in\ cylinder}}{stoichiometric\ ratio\ of\ combustion}$$

The stoichiometric ratio of combustion used in calculation is 0.08.

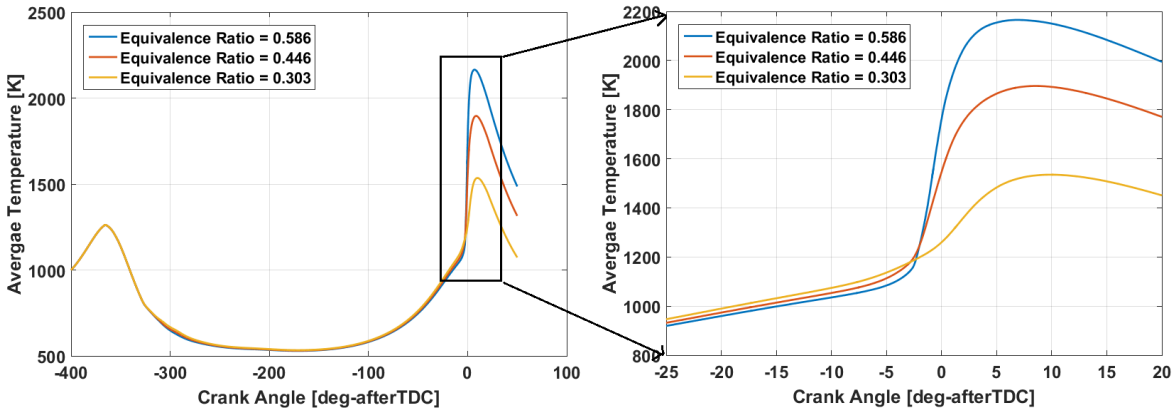

Figure 8. Effects of the equivalence ratio on the mixture temperature inside a cylinder

As Figure 8 shows, as the equivalence ratio increases, the maximum temperature inside the combustion chamber increases while the start of ignition advances. Additionally, as it is shown in Table 4, when the equivalence ratio is high, the combustion duration is significantly shortened. Since the HCCI burn rate is governed by chemical kinetics, the decomposition of H_2O_2 in particular, the amount of OH produced from the decomposition directly impacts the burn rate [20]. Therefore, once the temperature of the mixture reaches the decomposition temperature, the air-fuel mixture with a higher equivalence ratio can produce more OH than a

leaner mixture, which in turn accelerates its combustion process and results in higher burn rate. Consequently, the combustion duration is shortened for combustion with a richer mixture.

Table 4. Crank angles at different combustion phasing at three different equivalence ratios

Equivalence ratio	CA10 (crank angles)	CA50 (crank angles)	CA90 (crank angles)	Combustion duration (crank angles)	Total Heat release (J)
0.586	-2.46	-0.28	4.39	6.85	594.7
0.446	-2.91	0.02	6.31	9.22	441.9
0.303	-4.23	2.73	9.65	13.88	250.7

4. Summary

CFD simulations of the ignition and combustion processes in a single-cylinder HCCI engine are presented. The physical modeling used for the simulation includes: RANS turbulence modeling, a dynamic drag model to determine the drag coefficients of fuel droplets, the KH-RT spray breakup model and NTC methods for droplet collisions. Trends observed in the simulation agree with those in the experimental measurements. Intake temperature, cylinder wall temperature and equivalence ratio were changed individually to investigate their effects on combustion. The simulation results show that lower intake temperature and cylinder wall temperature retards ignition timing and extends ignition duration. The temperature of the charged mixture is found to be more sensitive to the temperature of cylinder walls than intake temperature. For lean mixtures, where the equivalence ratio is smaller than 1, the ignition of iso-octane is advanced as the equivalence ratio increases.

5. References

[1] J. Merkisz, J. Pielecha and S. Radzimirski, New trends in emission control in the European Union, Springer International PU, 2014.

[2] "Electric vehicles: not so fast," *IEEE Spectrum,* vol. 54, no. 12, p. 24, 2017.

[3] S. Saxena and I. Bedoya, "Fundamental phenomena affecting low temperature combustion and HCCI engines, high load limits and strategies for extending these limits," *Progress in Energy and Combustion Science,* vol. 39, no. 5, pp. 457-488, 2013.

[4] Commission of the European Communities. Proposal for a Regulation of the European Parliament and of the Council: Setting emission performance standards for new passenger cars and for new light commercial vehicles as part of the Union's integrated approach to reduce CO2 emissions from light-duty vehicles and amending Regulation. COM (2017) 676 final, 2017/0293 (COD), Brussels (2017)

[5] R. Ebrahimi and B. Desmet, "An experimental investigation on engine speed and cyclic dispersion in an HCCI engine", Fuel, vol. 89, no. 8, pp. 2149-2156, 2010.

[6] A. Iijima, H. Shoji, Y. Yoshida, C. Rin, M. Yamada, T. Shimada and N. Ito, "A Study of the Behavior of In-Cylinder Pressure Waves under HCCI Knocking by using an Optically Accessible Engine", SAE International Journal of Engines, vol. 9, no. 1, pp. 1-10, 2018.

[7] B. Lawler, S. Mamalis, S. Joshi, J. Lacey, O. Guralp, P. Najt and Z. Filipi, "Understanding the effect of operating conditions on thermal stratification and heat release in a homogeneous charge compression ignition engine", Applied Thermal Engineering, vol. 112, pp. 392-402, 2017.

[8] B. Moxey, A. Cairns and H. Zhao, "A Comparison of Burning Characteristics of Iso-Octane

ahnd Ethanol Fuels in an Optical SI Engine", Journal of KONES Powertrain and Transport, vol. 20, no. 2, pp. 299-305, 2013.

[9] Richards, K. J., Senecal, P. K., and Pomraning, E., CONVERGE 2.4 Manual, Convergent Science, Inc., Madison, WI (2017)

[10] Senecal, P.K., Richards, K.J., Pomraning, E., Yang, T., Dai, M.Z., McDavid, R.M., Patterson, M.A., Hou, S., and Shethaji, T., "A New Parallel Cut-Cell Cartesian CFD Code for Rapid Grid Generation Applied to In-Cylinder Diesel Engine Simulations," SAE Paper 2007-01-0159, 2007. DOI: 10.4271/2007-01-0159

[11] M. Huang, S. Gowdagiri, X. Cesari and M. Oehlschlaeger, "Diesel engine CFD simulations: Influence of fuel variability on ignition delay", Fuel, vol. 181, pp. 170-177, 2016.

[12] Anthony, C. Iannetti and Moder, P. Jeffrey, "Comparing spray characteristics from Reynolds Averaged Navier-Stokes (RANS) National Combustion Code (NCC) calculations against experimental data for a turbulent reacting flow", NASA technical memorandum, 216735.

[13] A. d'Adamo, S. Breda, S. Fontanesi, A. Irimescu, S. Merola and C. Tornatore, "A RANS knock model to predict the statistical occurrence of engine knock", Applied Energy, vol. 191, pp. 251-263, 2017.

[14] F. Bottone, A. Kronenburg, D. Gosman and A. Marquis, "Large Eddy Simulation of Diesel Engine In-cylinder Flow", Flow, Turbulence and Combustion, vol. 88, no. 1-2, pp. 233-253, 2011.

[15] Liu AB, Mather DK, Reitz RD. Modeling the effects of drop drag and breakup on fuel

sprays. SAE paper no. 930072; 1993.

[16] Som S, Senecal PK, Pomraning E. Comparison of RANS and LES turbulence models against constant volume diesel experiments. In: 24th annual conference on liquid atomization and spray systems.

[17] Schmidt, D.P. and Rutland, C.J., "A New Droplet Collision Algorithm," Journal of Computational Physics, 164(1), 62-80, 2000. DOI: 10.1006/jcph.2000.6568

[18] O’ Rourke, P.J., "Collective Drop Effects on Vaporizing Liquid Sprays," Ph.D. Thesis,Princeton University, Princeton, NJ, United States, 1981.

[19] Y. Liu, M. Jia, M. Xie and B. Pang, "Enhancement on a Skeletal Kinetic Model for Primary Reference Fuel Oxidation by Using a Semidecoupling Methodology", Energy & Fuels, vol. 26, no. 12, pp. 7069-7083, 2012.

[20] X. Lü, W. Chen and Z. Huang, "A fundamental study on the control of the HCCI combustion and emissions by fuel design concept combined with controllable EGR. Part 1. The basic characteristics of HCCI combustion", Fuel, vol. 84, no. 9, pp. 1074-1083, 2005.